

Mechanisms of DNA-mediated allostery

Midas Segers,¹ Aderik Voorspoels,¹ Takahiro Sakaue,² and Enrico Carlon¹

¹*Soft Matter and Biophysics, KU Leuven, Celestijnenlaan 200D, 3001 Leuven, Belgium*

²*Department of Physics and Mathematics, Aoyama Gakuin University,
5-10-1 Fuchinobe, Chuo-ku, Sagami-hara, Kanagawa 252-5258, Japan*

(Dated: January 11, 2024)

Proteins often regulate their activities via allostery - or action at a distance - in which the binding of a ligand at one binding site influences the affinity for another ligand at a distal site. Although less studied than in proteins, allosteric effects have been observed in experiments with DNA as well. In these experiments two or more proteins bind at distinct DNA sites and interact indirectly with each other, via a mechanism mediated by the linker DNA molecule. We develop a mechanical model of DNA/protein interactions which predicts three distinct mechanisms of allostery. Two of these involve an enthalpy-mediated allostery, while a third mechanism is entropy driven. We analyze experiments of DNA allostery and highlight the distinctive signatures allowing one to identify which of the proposed mechanisms best fits the data.

The term ‘‘allostery’’ indicates an action at a distance in biological macromolecules where the binding of a ligand at one site modifies the binding of another ligand at a distinct site. Many proteins regulate their activities via allostery [1], through mechanisms that are not fully understood and presently debated, see e.g. [2]. Although hitherto most of the focus has been on proteins, allosteric effects have been observed in DNA as well [3, 4] and discussed in models and simulations [5–7]. In DNA allostery two or more proteins binding at distinct sites interact with each other through some signal carried by the linker DNA, see Fig. 1(a). Experiments show that the interaction is weakly dependent on the DNA sequence [3, 4], suggesting that allostery may be described by a homogenous DNA model. The interaction is strongly attenuated if one of the two strands is cut (DNA nicking), which shows that allostery requires an intact DNA molecule. This and other experimental evidences [3, 4] show that the interaction is transmitted through DNA, and not via direct (electrostatic) or solvent-mediated effects. A model of force-induced allostery was discussed in [8]. However, this mechanism does not apply to experiments in which DNA is not under tension [3, 4].

In all generality, the total free energy for the system consisting of DNA and two bound proteins, separated by a linker sequence of m base pairs, is

$$F_{ab} = F_0 + \Delta F_a + \Delta F_b + \Delta\Delta F_{int}(m) \quad (1)$$

where F_0 is the bulk contribution from DNA in absence of bound proteins, ΔF_a and ΔF_b are the excess free energies when only one of the two proteins, either ‘‘a’’ or ‘‘b’’, is bound. The interaction term, $\Delta\Delta F_{int}(m)$, is the excess free energy when both proteins are bound which vanishes as $m \rightarrow \infty$. If $\Delta\Delta F_{int} < 0$ the simultaneous binding of the two proteins leads to a net decrease of the total free energy (cooperative binding). If $\Delta\Delta F_{int} > 0$, the simultaneous binding is destabilized. We introduce a model which predicts three distinct mechanisms of allostery, corresponding to different forms of $\Delta\Delta F_{int}$. We introduce collective variables X_n at each base pair position $0 \leq n < N$, which are local reaction coordinates

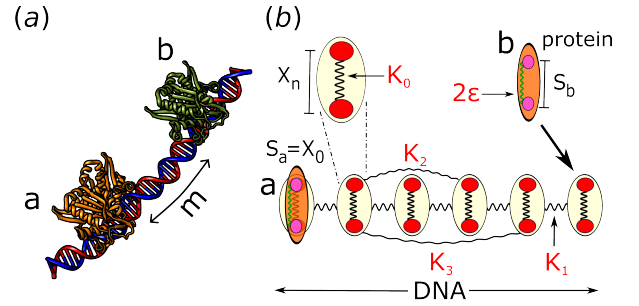


FIG. 1. (a) DNA-mediated interaction for two bound proteins separated by a linker molecule of m base pairs. (b) Model of DNA allostery. The DNA substrate (yellow) is described as a set of variables $X_n \equiv u_n + \bar{l}$ defined at each base-pair site, with $\langle X_n \rangle = \bar{l}$ the equilibrium value. These variables are characterized by a local stiffness (K_0) and distal couplings (K_1, K_2, \dots), with energy given by (2). Upon binding, the protein (orange blob) modifies the local mechanical properties of the DNA substrate. The distal couplings carry the signal to distinct sites. The schematic plot in (b) shows a protein interacting with a single DNA site. The more realistic case of proteins binding to several DNA sites is also considered.

associated to DNA-protein binding. We define $\bar{l} \equiv \langle X_n \rangle$, the equilibrium value, and $u_n \equiv X_n - \bar{l}$. At base pair level, DNA deformations are described by several coarse-grained coordinates like the 12 canonical ones (twist, roll, tilt, rise, ...) of the rigid base model [9]. In our model u_n could be one of these coordinates, a combination thereof, or any other local deformation parameter. Experimental data, discussed further, put constraints on the properties of u_n which gives insights on candidate allostery-carrying variables. In the u_n the energy of free DNA is

$$H_0 = \frac{1}{2} \sum_{n=0}^{N-1} \left[K_0 u_n^2 + \sum_{p=1}^L K_p (u_n u_{n+p} + u_n u_{n-p}) \right] \quad (2)$$

which is quadratic with local stiffness K_0 and distal couplings $K_p u_n u_{n+p}$ (Fig. 1(b)) here assumed to extend to a finite range L . Distal couplings naturally arise from the

collective nature of u_n and are indeed observed in simulations [10–14]. They typically extend to a few flanking nucleotides (truncated at a distance L in (2)) and the strength and decay of the interactions depend on the coarse-grained variable considered [13]. Distal couplings are essential to generate allostery. The model (2) is coarse-grained with one degree of freedom per DNA site and it can be solved analytically. Using periodic boundary conditions ($u_N \equiv u_0$) we write (2) as

$$H_0 = \frac{1}{2N} \sum_q \tilde{K}_q |\mathcal{U}_q|^2 \quad (3)$$

where we introduced the discrete Fourier transforms

$$\mathcal{U}_q = \sum_{n=0}^{N-1} e^{-2\pi i n q / N} u_n, \quad \tilde{K}_q = \sum_{n=-L}^L K_n \cos\left(\frac{2\pi n q}{N}\right) \quad (4)$$

with q an integer, $K_{-p} = K_p$ and $-N/2 < q < N/2$ [15]. In absence of distal couplings ($K_p = 0$ for $p \geq 1$) the q -stiffness $\tilde{K}_q = K_0$ is constant, thus a q -dependence of \tilde{K}_q reflects the existence of couplings between distal sites. Note that the couplings K_p can take any value as long as $\tilde{K}_q > 0$ for real q (stability condition).

We consider first proteins interacting with a single DNA site. An unbound protein is thus described by a single collective variable S , with average $\langle S \rangle = \bar{s}$ and energy $H_p = \varepsilon(S - \bar{s})^2$. The binding to DNA (at site $n = 0$) forces the corresponding collective variables to assume the same value $S = X_0 = \bar{l} + u_0$ so that the total energy of DNA and protein ($H_0 + H_p$) takes the form

$$H = H_0 + \varepsilon [u_0^2 + 2(\bar{l} - \bar{s})u_0 + (\bar{l} - \bar{s})^2], \quad (5)$$

omitting a constant binding energy which does not influence $\Delta\Delta F_{int}$. Equation (5) shows that protein binding introduces perturbation “fields” proportional to u_0 and u_0^2 . If the equilibrium value of the collective coordinates of DNA and protein coincide ($\bar{s} = \bar{l}$), the linear term vanishes and only the term proportional to u_0^2 “survives” in (5). Conversely, if $|\bar{l} - \bar{s}|$ is large one can neglect the quadratic term contribution [16]. In the following we compute $\Delta\Delta F_{int}$ for three different cases where the proteins induces a linear or a quadratic field.

A quantity of central interest is the propagator

$$S_m \equiv \frac{1}{N} \sum_q \frac{e^{2\pi i m q / N}}{\tilde{K}_q} = \beta \langle u_0 u_m \rangle_0, \quad (6)$$

where $\beta = 1/k_B T$ is the inverse temperature and $\langle \cdot \rangle_0$ indicates a thermal average with respect of H_0 . Equation (6) follows from the equipartition theorem

$$\beta \langle \mathcal{U}_q \mathcal{U}_p \rangle_0 = N \tilde{K}_q^{-1} \delta_{q,-p}. \quad (7)$$

Transforming the sum in (6) into an integral ($N \rightarrow \infty$ limit), one obtains the asymptotic behavior of S_m from

the leading pole, i.e. the solution of $\tilde{K}_q = 0$ with the smallest imaginary part. This equation cannot have solutions for real q as stability requires $\tilde{K}_q > 0$. In the most general case the leading pole has real and imaginary parts. Since \tilde{K}_q is real for real q and symmetric in $\pm q$ (see (4)) there are at least four poles, one of which is

$$\frac{2\pi q_E}{N} \equiv \phi + \frac{i}{\xi_E} \quad (8)$$

and the others are $-q_E$, q_E^* and $-q_E^*$, where $*$ denotes complex conjugation. The asymptotic behavior is governed by q_E

$$S_m \stackrel{m \gg 1}{\sim} \Gamma \cos(m\phi + \phi_0) e^{-m/\xi_E} \quad (9)$$

with ϕ_0 a phase shift and Γ a scale factor [17].

Enthalpic allostery – We consider first

$$H^E = H_0 - h(u_0 + u_m) \quad (10)$$

with $h = -2\varepsilon(\bar{l} - \bar{s})$, following (5). We find [17]

$$\Delta\Delta F_{int}^E = -h^2 S_m \quad (11)$$

which, being temperature independent, describes an interaction of enthalpic origin [30]. The fields in 0 and m shift the equilibrium values of u_0 and u_m and the distal couplings K_1, K_2, \dots propagate this perturbation to flanking sites, leading to $\langle u_n \rangle \neq 0$. Asymptotically the interaction decays via damped oscillations, see (9). We refer to ξ_E in (9) as the enthalpic allosteric length. The interaction stabilizes or destabilizes the simultaneous protein binding depending on their distance m , see Fig. 2(a). The calculation can be generalized to protein-DNA couplings involving more than one site, i.e. of the type $\sum_{k=0}^{n_a-1} h_k u_k + \sum_{l=n_a-1}^{n_a+n_b-2} h_{m+l} u_{m+l}$ where n_a (n_b) are the number of sites to which first (second) protein binds and m is the number of base pairs separating the nearest edges of the two proteins. The asymptotic decay remains of the form (9) which is universal [17].

Entropic allostery – We consider next

$$H^S = H_0 + \varepsilon (u_0^2 + u_m^2) \quad (12)$$

Differently from the enthalpic case, here $\langle u_n \rangle = 0$ for all sites. We find [17]

$$\Delta\Delta F_{int}^S = \frac{k_B T}{2} \log \left[1 - \left(\frac{2\varepsilon S_m}{1 + 2\varepsilon S_0} \right)^2 \right] \quad (13)$$

The interaction is of entropic origin $\Delta\Delta F_{int}^S = -T\Delta\Delta S \leq 0$, implying a net increase in entropy when both proteins are bound (cooperative binding). This can be understood as follows. The local stiffening to $K_0 + 2\varepsilon$ at sites 0 and m induces an entropy reduction in two regions surrounding the two perturbed sites. When m is sufficiently small, the two regions overlap which leads to a net entropy gain, hence $\Delta\Delta S > 0$. This is reminiscent

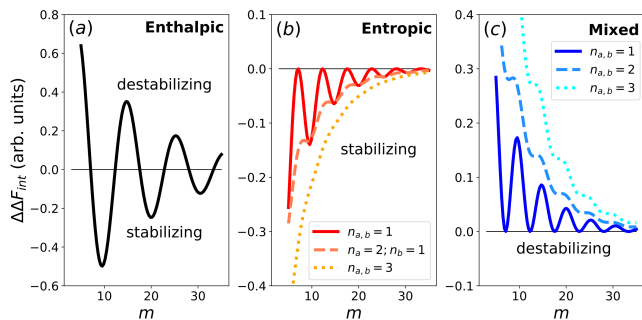


FIG. 2. Plots of $\Delta\Delta F_{int}$ vs. linker DNA length m for the three different mechanisms of DNA-mediated allostery proposed: (a) enthalpic, (b) entropic and (c) mixed. An angular frequency $\phi = 2\pi/10.5$, corresponding to the periodicity of the DNA double helix and $\xi_E = 15$ bp were used. These parameters match those observed in experiments (see Fig. (3)). In the case (a) the interaction is stabilizing/destabilizing depending on the values of m and the asymptotic oscillating behavior is universal, i.e. also valid for interactions involving n_a, n_b sites for protein a and b, respectively. In the cases (b) and (c) the interaction is always stabilizing and destabilizing, respectively. In (b) and (c) the asymptotic decay is non-universal, being dependent on the number of interacting sites $n_{a,b}$ per protein.

of entropic attractions observed in soft condensed matter systems, such as polymer-colloid mixtures [31]. In the limit $m \gg 1$, $\Delta\Delta F_{int}^S$ vanishes as S_m^2 . This implies (Eq. (9)) a decay length which is half of the enthalpic allosteric length $\xi_S = \frac{1}{2}\xi_E$, and an oscillating prefactor proportional to $\cos^2(m\phi + \phi_0)$, as shown in Fig. 2(b), red solid line. We extended the analysis of $\Delta\Delta F_{int}^S$ for protein-DNA contacts at more than one site. We consider first $\varepsilon(u_0^2 + u_1^2 + u_{m+1}^2)$, which can be solved analytically ([17], Eq. (S43)) shown as dashed line in Fig. 2(b). Unlike (13), this extended binding case contains terms proportional to S_m^2, S_{m+1}^2 and $S_m S_{m+1}$, each oscillating but with different phases. Figure 2(b) (dotted) shows $\Delta\Delta F_{int}^S$ for an interaction term $\varepsilon(\sum_{l=0}^2 u_l^2 + \sum_{k=m}^{m+2} u_k^2)$ in which each protein couples to a block of $3u$'s. There is in this case a very weak modulation of the exponential decay. Summarizing, the asymptotic behavior for generic quadratic interactions is

$$\Delta\Delta F_{int}^S \sim f(m) e^{-2m/\xi_E} \quad (14)$$

with a non-universal prefactor $f(m) \leq 0$, which depends on details of the protein-DNA bindings (unlike the universal behavior of the enthalpic case).

Mixed allostery - Finally, we consider the mixed case

$$H^M = H_0 - hu_0 + \varepsilon u_m^2 \quad (15)$$

for which we find [17]

$$\Delta\Delta F_{int}^M = \frac{\varepsilon h^2 S_m^2}{1 + 2\varepsilon S_0} \quad (16)$$

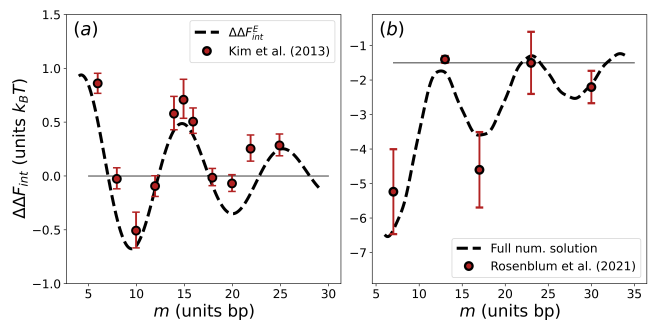


FIG. 3. (a) Symbols: Experimental data of interaction free energies for (BamHI-GRDBD) [3]. Oscillating sign in $\Delta\Delta F_{int}$ indicates an enthalpic type of allostery. Dashed line: Fit to the asymptotic expression (9) ($\phi = 2\pi/10.5$, $\xi_E = 15$ bp). (b) Symbols: Experimental data for $\Delta\Delta F_{int}$ for the ComK system [4]. The negative sign indicates an allosteric interaction which is of predominant entropic. Dashed line: Full numerical solution of $\Delta\Delta F_{int}(m)$ ($\phi = 2\pi/10.5$, $\xi_E = 22$ bp) for a global allostery model with extended perturbations [17]. As $\Delta\Delta F_{int}$ does not seem to converge to zero for large m , we have added an asymptotic non-zero offset (dotted line).

which is positive and thus a destabilizing interaction term. It is temperature independent and thus of enthalpic nature. The term $-hu_0$ produces a $\langle u_n \rangle \neq 0$, which contributes to the enthalpic part, but we find no entropy change in this model. As $\Delta\Delta F_{int}^M$ depends on S_m^2 the asymptotic is very similar to the entropic case, with decay length $\xi_M = \frac{1}{2}\xi_E$ and oscillations proportional to $\cos^2(m\phi + \phi_0)$. As in the entropic case, interactions to more than one site lead to a decay of the type (14), with $f(m) \geq 0$. We note that (11) and (13) (but not (16)) were also derived in a study of interactions of point defects in fluctuating membranes [32]. Their applicability is general and not limited to a one dimensional chain.

Experiments - In principle, one could distinguish the three scenarios in experiments from the sign of $\Delta\Delta F_{int}$ (Fig. 2). Kim *et al.* analyzed the binding of several different pairs of proteins on DNA [3]. The binding free energy showed a decaying oscillating behavior with alternating sign which is consistent with an enthalpic allostery (10), in agreement with the analysis performed by other authors [3, 5, 6, 33]. A fit to (10) with the asymptotic expression for S_m (9) is shown in Fig. 3(a). A different system was analyzed by Rosenblum *et al.* [4] who found DNA-mediated allostery in the binding of bacterial transcription factors ComK. The experiments showed a cooperative binding ($\Delta\Delta F_{int} < 0$) for varying spacer lengths, see Fig. 3(b). The negative $\Delta\Delta F_{int}$ indicates an allostery of (predominantly) entropic type. The data are fitted (dashed line) against a model containing both linear and quadratic terms, using a Monte Carlo fitting procedure [17]. These fields act on several sites reflecting the extended contact regions of the ComK-DNA interaction. The oscillating component is due to the enthalpic part, which, as seen above, has a universal oscillatory de-

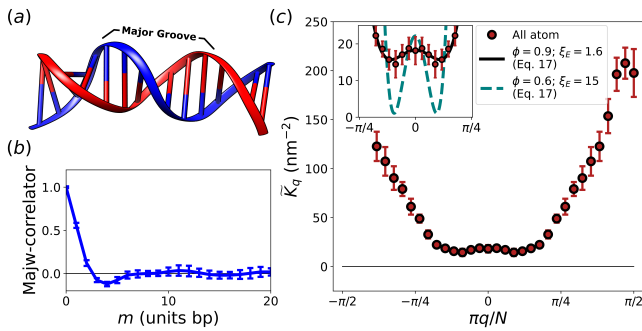


FIG. 4. (a) Schematic representation of the major groove width of DNA, in practice the Curves+ [35] definition is used. (b) Correlation function of the major groove width as obtained from all-atom simulations obtained using the Curves+ software [35]. (c) Plot of the momentum-space stiffness for the major groove width obtained from all-atom data. The inset coplots \tilde{K}_q for the minimal model (Eq. (17)) for two sets of parameters. The solid line is a direct fit of the stiffness data. The dashed line uses ϕ and ξ_E from a fit of the experimental $\Delta\Delta F_{int}$ data. The error-bars in (b) and (c) indicate the standard deviation calculated over 21 time windows of 10 ns.

caying behavior. In the fit the same value of $\phi = 2\pi/10.5$ as Fig. 3(a) was used. Instead for the correlation length we used $\xi_E = 22$ bp, larger than the value used in (a), possibly indicating that allosteric coupling is carried over by different collective variables in the two cases. We note that the ComK have much larger $|\Delta\Delta F_{int}|$ than the data shown in Fig. 3(a). It is possible that to quantitatively describe the ComK data one would need to go beyond linear elasticity (anharmonic effects) or to more complex multimodal models [34]. However, the harmonic model with linear and quadratic terms spanning several sites generates a $\Delta\Delta F_{int}$ consistent with experimental data.

Simulations - So far we have assumed a model with distal couplings generating allosteric interactions, using a generic u_n . In principle u_n could be one of the several DNA local deformation modes used in the rigid base model [9], or a combination thereof. However, experiments indicate that allosteric interactions decay via damped oscillations, which puts some constraints on u_n , as several variables do not have this property. For instance, we can exclude pure bending or twist modes as candidates for u_n , as the stiffness \tilde{K}_q for these coordinates does not produce oscillations with the desired periodicity [17]. Prior work suggested the DNA major groove width as mediating allosteric interactions [3]. However, extensive 1 μ s all-atom simulations of a 33-bp sequence showed no signature of periodicity in the groove width correlations [33]. We have performed simulations using two different 44-bp sequences for 100 ns, with major groove width calculated from the algorithm Curves+ [35] using the setup discussed in [13]. Our results for the normalized propagator $S_m/S_0 = \langle u_0 u_m \rangle_0 / \langle u_0^2 \rangle_0$ (with u_n the deviation of the major groove width from the equilibrium value) are given in Fig. 4(b) and are in close agreement

with those reported in [33]. To extract parameters from simulations we have calculated the q -stiffness \tilde{K}_q from the equipartition relation (7), as recently done for twist and bending deformations [13, 36]. A minimal model with just four poles $\pm q_E, \pm q_E^*$ (8) gives

$$\tilde{K}_q = A(q^2 - q_E^2)(q^2 - q_E^{*2}) = A(q^4 - \mu q^2 + \lambda^2) \quad (17)$$

with A a scale factor, $\mu = q_E^2 + q_E^{*2}$ and $\lambda = |q_E|^2$. We note that (17) is not of the form (4), but should be interpreted as the continuum long wavelength limit ($q \rightarrow 0$) of model (2). Figure 4(c) shows \tilde{K}_q as obtained from simulation data averaged over two sequences (red circles). The double-well shaped curve is fitted, for small q , to (17) giving $\phi = 0.9$ and $\xi_E = 1.6$ (solid line in the inset of Fig. 4). The former parameter is close to the double helix periodicity $\phi = 2\pi/10.5 \approx 0.6$, while the latter appears to be quite small as compared to experimental data which predict $\xi_E \approx 15$ bp. We show on the same inset a plot of Eq. (17) with the latter values for ϕ and ξ_E . We conclude that simulations of the major-groove width qualitatively support the distal couplings model (2), but a quantitative matching remains an open challenge, as pointed out earlier [7, 33]. See [17] for an extended discussion on possible origins of these discrepancies.

Conclusions - We have studied a coarse-grained model which predicts three types of allosteric DNA-mediated interactions. One could distinguish between the three cases (or about the dominance of one of these) from the sign of the interaction free energy and on its dependence on the length of the DNA linker sequence separating the two protein-binding sites. Prior work [3, 5, 6] pointed to some examples of enthalpic DNA-mediated allostery characterized by a free energy of oscillating sign. We have argued here that recent ComK data [4] show an allostery which is of predominant entropic nature, as $\Delta\Delta F_{int} < 0$. Entropic allostery (often referred as dynamic allostery) was discussed in the case of proteins [37, 38], but it should manifest itself in DNA as well. The model introduced here predicts additionally a “mixed” allostery, obtained when coupling two different proteins in which one exerts a linear field and the other a quadratic one. This mixed allostery is of enthalpic nature and we are not aware that such interaction was discussed in the protein literature. Differently from the protein case, in DNA-mediated allostery one can vary the spacer sequence length, probing the decay of $\Delta\Delta F_{int}$, therefore the type of allostery (enthalpic, entropic or mixed) should be easier to identify. By varying the binding sites sequences one can bring in close vicinity proteins of different types and which couple differently to the DNA (e.g. predominantly via linear or quadratic fields), thereby probing the three scenarios predicted by the model.

MS acknowledges financial support from Fonds Wetenschappelijk Onderzoek (FWO 1102323N). EC thanks the Aoyama-Gakuin University (Japan) and Laboratoire C. Coulomb of the University of Montpellier (France), where part of this work was done, for the kind hospitality. He

acknowledges financial support from the Japan Society for the Promotion of Science (FY2020 JSPS). Discus-

sions with G. Bussi, H. Hofmann and G. Rosenblum are gratefully acknowledged.

-
- [1] K. Gunasekaran, B. Ma, and R. Nussinov, *Proteins* **57**, 433 (2004).
- [2] S. J. Wodak *et al.*, *Structure* **27**, 566 (2019).
- [3] S. Kim *et al.*, *Science* **339**, 816 (2013).
- [4] G. Rosenblum *et al.*, *Nature Comm.* **12**, 1 (2021).
- [5] T. Dršata *et al.*, *J. Phys. Chem. Lett.* **5**, 3831 (2014).
- [6] J. Singh and P. K. Purohit, *J. Phys. Chem. B* **123**, 21 (2018).
- [7] A. Balaceanu, A. Pérez, P. D. Dans, and M. Orozco, *Nucl. Acids Res.* **46**, 7554 (2018).
- [8] J. Rudnick and R. Bruinsma, *Biophys. J.* **76**, 1725 (1999).
- [9] W. K. Olson *et al.*, *J. Mol. Biol.* **313**, 229 (2001).
- [10] F. Lankaš, J. Šponer, P. Hobza, and J. Langowski, *J. Mol. Biol.* **299**, 695 (2000).
- [11] A. Noy and R. Golestanian, *Phys. Rev. Lett.* **109**, 228101 (2012).
- [12] B. Eslami-Mossallam and M. Ejtehadi, *J. Chem. Phys.* **134**, 03B623 (2011).
- [13] E. Skoruppa, A. Voorspoels, J. Vreede, and E. Carlon, *Phys. Rev. E* **103**, 042408 (2021).
- [14] Y. A. G. Fosado, F. Landuzzi, and T. Sakaue, *Phys. Rev. Lett.* **130**, 058402 (2023).
- [15] Models as (2) were used in the literature to describe large scale packing of chromosomal DNA, see A. Amitai and D. Holzman, *Phys. Rev. E* **88**, 052604 (2013) and K. Polovnikov, S. Nechaev, and M. Tamm, *Soft Matter* **14**, 6561 (2018). Some of these models considered a slowly algebraic decay of the off-site couplings $K_p \sim p^{-a}$ (and $L \rightarrow \infty$), which gives a Fourier space stiffness \tilde{K}_q non-analytic in $q = 0$. We consider here couplings extending to a finite range L , hence such non-analytic behavior will not occur.
- [16] The linear term is dominant when $|l_0 - s_0|^2 \gg \langle u_0^2 \rangle_0$.
- [17] See Supplemental material at <http://>, which contains references [18–29], for details of mathematical derivations, simulations and additional information about the models used.
- [18] F. Lankaš *et al.*, *Phys. Chem. Chem. Phys.* **11**, 10565 (2009).
- [19] A. Voorspoels, J. Vreede, and E. Carlon, *J. Chem. Theor. Comp.* **19**, 902 (2023).
- [20] D. Petkevičiūtė, M. Pasi, O. Gonzalez, and J. Maddocks, *Nucl. Acids Res.* **42**, e153 (2014).
- [21] M. Abrahams *et al.*, *SoftwareX* **1-2**, 19 (2015).
- [22] A. Perez *et al.*, *Biophys. J.* **92**, 3817 (2007).
- [23] I. Ivani *et al.*, *Nat. Methods* **13**, 55 (2016).
- [24] W. L. Jorgensen, J. Chandrasekhar, J. D. Madura, R. W. Impey, and M. L. Klein, *J. Chem. Phys.* **79**, 926 (1983).
- [25] S. Li, W. Olson, and X.-J. Lu, *Nucl. Acids Res.* **47**, W26 (2019).
- [26] G. Bussi, D. Donadio, and M. Parrinello, *J. Chem. Phys.* **126**, 014101 (2007).
- [27] M. Parrinello and A. Rahman, *J. Appl. Phys.* **52**, 7182 (1981).
- [28] B. Hess, H. Bekker, H. J. C. Berendsen, and J. G. E. M. Fraaije, *J. Comput. Chem.* **18**, 1463 (1997).
- [29] K. Liebl and M. Zacharias, *Biophys. J.* **122**, 2841 (2023).
- [30] The coarse-grained variables u_n derive from an underlying partial integration of microscopic degrees of freedom. This may lead to a temperature dependence of the couplings K_n . Here enthalpic/entropic interactions refer to this coarse-grained level of description. Our focus is on the sign of $\Delta\Delta F_{int}$ rather than its temperature dependence.
- [31] T. Witten and P. Pincus, *Structured Fluids: Polymers, Colloids, Surfactants* (OUP Oxford, 2010).
- [32] R. R. Netz, *J. de Physique I* **7**, 833 (1997).
- [33] T. Dršata, M. Zgarbová, P. Jurečka, J. Šponer, and F. Lankaš, *Biophys. J.* **110**, 874 (2016).
- [34] K. López-Güell, F. Battistini, and M. Orozco, *Nucl. Acids Res.* **51**, 2633 (2023).
- [35] R. Lavery *et al.*, *Nucl. Acids Res.* **37**, 5917–5929 (2009).
- [36] M. Segers, A. Voorspoels, T. Sakaue, and E. Carlon, *J. Chem. Phys.* **156**, 234105 (2022).
- [37] R. J. Hawkins and T. C. McLeish, *Phys. Rev. Lett.* **93**, 098104 (2004).
- [38] N. V. Dokholyan, *Chem. Rev.* **116**, 6463 (2016).

**SUPPLEMENTAL INFORMATION M. SEGERS
ET AL. "MECHANISMS OF DNA-MEDIATED
ALLOSTERY"**

This document is organized as follows. Section I shows the details of the calculations of the exact expressions of the interaction free energy $\Delta\Delta F_{int}$ for enthalpic (IB), entropic (IC) and mixed (ID) allostery. These are given in the framed equations (33), (40) and (46) and are expressed as functions of the propagator S_m . These results are derived for pointwise interactions at two single sites and are generalized to the case of proteins interacting to multiple sites in IF. Section II discusses the asymptotic behavior of the propagator, the allosteric length and its connection with DNA persistence lengths. Section III gives some details of the procedure followed to fit the ComK data. Section IV discusses details of all-atom simulations.

**I. ENTHALPIC, ENTROPIC AND MIXED
ALLOSTERY**

A. Correlation functions in free DNA

Let us consider the free DNA model as given by (2) in the main text. The equilibrium probability distribution $p(u_0, u_1 \dots u_{N-1})$, due to the quadratic nature of the interactions, is a multivariate gaussian distribution. Integrating all variables but u_0 and u_m gives a joint probability distribution for u_0 and u_m which is still gaussian

$$p(u_0, u_m) \sim e^{-A(u_0^2 + u_m^2) - 2Bu_0u_m} \quad (18)$$

with A and B some coefficients. From integration of (18) we find

$$\langle u_0 u_m \rangle_0 = -\frac{1}{2} \frac{B}{A^2 - B^2} \quad (19)$$

$$\langle u_0^2 \rangle_0 = \frac{1}{2} \frac{A}{A^2 - B^2} \quad (20)$$

where we used the subscript "0" to stress that these are correlations of free DNA in absence of perturbing fields. Using the inverse Fourier transform

$$u_n = \frac{1}{N} \sum_{q=0}^{N-1} e^{2\pi i q n / N} \mathcal{U}_q, \quad (21)$$

we can compute the correlations directly

$$\begin{aligned} \langle u_0 u_m \rangle_0 &= \frac{1}{N^2} \sum_{q, q'} e^{2\pi i m q / N} \langle \mathcal{U}_q \mathcal{U}_{q'} \rangle_0 \\ &= \frac{k_B T}{N} \sum_q \frac{e^{2\pi i m q / N}}{\tilde{K}_q} = k_B T S_m \end{aligned} \quad (22)$$

where the propagator S_m follows the same definition of the main text (6). To obtain (22) we have used the

equipartition relation

$$\langle \mathcal{U}_q \mathcal{U}_{q'} \rangle_0 = N k_B T \tilde{K}_q^{-1} \delta_{q, -q'} \quad (23)$$

Setting $m = 0$ in (22) we get

$$\langle u_0^2 \rangle_0 = \frac{k_B T}{N} \sum_q \frac{1}{\tilde{K}_q} = k_B T S_0 \quad (24)$$

Comparing (19), (20) with (22), (24) we obtain the following expressions for A and B

$$A = \frac{\beta}{2} \frac{S_0}{S_0^2 - S_m^2} \quad (25)$$

$$B = \frac{\beta}{2} \frac{-S_m}{S_0^2 - S_m^2} \quad (26)$$

B. Enthalpic allostery

We use (18) and the expressions for A and B (25), (26) to compute the interaction free energy for enthalpic allostery. The partition function of the free system (DNA with no proteins bound) is

$$Z_0 = \int \frac{du_0 du_m}{\pi} e^{-A(u_0^2 + u_m^2) - 2Bu_0u_m} = \frac{1}{\sqrt{A^2 - B^2}} \quad (27)$$

where we divided by π for convenience. The bulk free energy is then

$$F_0 = -k_B T \log Z_0 = \frac{k_B T}{2} \log (A^2 - B^2) \quad (28)$$

Inserting a protein at site u_0 gives the partition function

$$\begin{aligned} Z_a &= \int \frac{du_0 du_m}{\pi} e^{-A(u_0^2 + u_m^2) - 2Bu_0u_m} e^{\beta h u_0} \\ &= \frac{1}{\sqrt{A^2 - B^2}} \exp \left[\frac{\beta^2 h^2 A}{4(A^2 - B^2)} \right] \\ &= Z_0 \exp \left[\frac{\beta^2 h^2 A}{4(A^2 - B^2)} \right] \end{aligned} \quad (29)$$

which, using $-k_B T \log Z_a = F_0 + \Delta F_a$ and (28), gives the following excess free energy for a single bound protein

$$\Delta F_a = -\frac{\beta h^2}{4} \frac{A}{A^2 - B^2} \quad (30)$$

The partition function of two bound proteins is then

$$\begin{aligned} Z_{ab} &= \int \frac{du_0 du_m}{\pi} e^{-A(u_0^2 + u_m^2) - 2Bu_0u_m} e^{\beta h(u_0 + u_m)} \\ &= \frac{1}{\sqrt{A^2 - B^2}} \exp \left[\frac{\beta^2 h^2}{2(A + B)} \right] \end{aligned} \quad (31)$$

Using the relation

$$F_0 + \Delta F_a + \Delta F_b + \Delta\Delta F_{int} = -k_B T \log Z_{ab} \quad (32)$$

with (28) and (37) (in our calculation the bound proteins are assumed to be identical $\Delta F_a = \Delta F_b$) we get the following estimate of the interaction free energy

$$\boxed{\Delta\Delta F_{int}^E = \frac{\beta h^2}{2} \frac{B}{A^2 - B^2} = -h^2 S_m} \quad (33)$$

where we have used Eqs. (25) and (26) to obtain the final result as a function of S_m .

C. Entropic allostery

We consider now the model for entropic allostery

$$H = H_0 + \varepsilon (u_0^2 + u_m^2) \quad (34)$$

and compute the interaction free energy $\Delta\Delta F_{int}^S$ as a function of the parameters A and B as done above for enthalpic allostery. The partition function for a system with a single protein bound is

$$\begin{aligned} Z_a &= \int \frac{du_0 du_m}{\pi} e^{-A(u_0^2 + u_m^2) - 2Bu_0 u_m} e^{-\beta \varepsilon u_0^2} \\ &= \frac{1}{\sqrt{A(A + \beta \varepsilon) - B^2}} \end{aligned} \quad (35)$$

from which one can calculate the excess free energy due to the bound protein

$$F_0 + \Delta F_a = -k_B T \log Z_a = \frac{k_B T}{2} \log [A(A + \beta \varepsilon) - B^2] \quad (36)$$

Subtracting the expression for F_0 in (28) one gets the excess free energy associated to a single isolated protein

$$\Delta F_a = \frac{k_B T}{2} \log \frac{A(A + \beta \varepsilon) - B^2}{A^2 - B^2} \quad (37)$$

The partition function for two bound proteins is

$$Z_{ab} = \int \frac{du_0 du_m}{\pi} e^{-A(u_0^2 + u_m^2) - 2Bu_0 u_m} e^{-\beta \varepsilon (u_0^2 + u_m^2)} \quad (38)$$

from which one gets the total free energy

$$F_0 + 2\Delta F_a + \Delta\Delta F_{int}^S = \frac{k_B T}{2} \log [(A + \beta \varepsilon)^2 - B^2] \quad (39)$$

Subtracting from the previous expression (28) and (37) one obtains for the interaction free energy

$$\begin{aligned} \Delta\Delta F_{int}^S &= \frac{k_B T}{2} \log \frac{[(A + \beta \varepsilon)^2 - B^2] (A^2 - B^2)}{[A(A + \beta \varepsilon) - B^2]^2} \\ &= \frac{k_B T}{2} \log \left[1 - \left(\frac{2\varepsilon S_m}{1 + 2\varepsilon S_0} \right)^2 \right] \end{aligned} \quad (40)$$

where we have used the expressions for A and B (25), (26). There is no temperature dependence in the argument of the logarithm in (40), showing indeed that the interaction free energy is of purely entropic nature

$$\Delta\Delta F_{int}^S = -T \Delta\Delta S_{int} \quad (41)$$

D. Mixed (enthalpic) allostery

We repeat the analysis for the mixed case

$$H = H_0 + \varepsilon u_0^2 - h u_m \quad (42)$$

in which one protein induces a linear perturbation field, while the other a quadratic one. This implies that the two proteins must be different, as they interact with DNA in a substantial different way at the two binding sites. The isolated proteins excess free energies were already calculated previously and are given by Eqs. (30) and (37), respectively:

$$\Delta F_a + \Delta F_b = -\frac{\beta h^2 A}{4(A^2 - B^2)} + \frac{k_B T}{2} \log \frac{A(A + \beta \varepsilon) - B^2}{A^2 - B^2} \quad (43)$$

The partition function for two bound proteins is

$$\begin{aligned} Z_{ab} &= \int \frac{du_0 du_m}{\pi} e^{-A(u_0^2 + u_m^2) - 2Bu_0 u_m} e^{-\beta(\varepsilon u_0^2 + h u_m)} \\ &= \frac{1}{\sqrt{A(A + \beta \varepsilon) - B^2}} \exp \left(\frac{\beta^2 h^2}{4} \frac{A + \beta \varepsilon}{A(A + \beta \varepsilon) - B^2} \right) \end{aligned} \quad (44)$$

From the above expression

$$-k_B T \log Z_{ab} = F_0 + \Delta F_a + \Delta F_b + \Delta\Delta F_{int} \quad (45)$$

and using (28), (44) and (43) one gets

$$\begin{aligned} \Delta\Delta F_{int}^M &= \frac{\beta^2 h^2 \varepsilon}{4} \frac{B^2}{(A^2 - B^2) [A(A + \beta \varepsilon) - B^2]} \\ &= \frac{\varepsilon h^2 S_m^2}{1 + 2\varepsilon S_0} \end{aligned} \quad (46)$$

where the expressions (25) and (26) were used.

E. Global Allostery

In the most general case a protein will exert both a linear and a quadratic field. Here we consider the following model

$$H = H_0 + \varepsilon_a u_0^2 - h_a u_0 + \varepsilon_b u_m^2 - h_b u_m \quad (47)$$

using the same methodology as for the limiting cases above, we find the following interaction free energy

$$\begin{aligned} \Delta\Delta F_{int}(m) &= \frac{k_B T}{2} \log \left(1 - \frac{4\varepsilon_a \varepsilon_b S_m^2}{(1 + 2\varepsilon_a S_0)(1 + 2\varepsilon_b S_0)} \right) \\ &\quad - \frac{h_a h_b S_m}{1 + 2(\varepsilon_a + \varepsilon_b) S_0} \\ &\quad + \frac{\varepsilon_a h_b^2 S_m^2}{(1 + 2(\varepsilon_a + \varepsilon_b) S_0)(1 + 2\varepsilon_b S_0)} \\ &\quad + \frac{\varepsilon_b h_a^2 S_m^2}{(1 + 2(\varepsilon_a + \varepsilon_b) S_0)(1 + 2\varepsilon_a S_0)} \end{aligned} \quad (48)$$

The first term comprises the entropic contribution, whereas the latter three are purely of an enthalpic nature. The second term couples the two linear fields h_a and h_b similar to (33), whereas the third and last term are the equivalent of mixed allostery (see (46)).

F. Extended DNA-protein couplings

Thus far we have discussed the effect of proteins on a single local site. In general a protein will interact with a few DNA sites and we discuss here the case of extended DNA-protein couplings.

1. Enthalpic allostery: robustness of oscillating decay

We consider first the case of linear perturbations and consider the following model

$$H = H_0 - \sum_{k=0}^{n_a-1} h_k u_k - \sum_{l=n_a-1}^{n_a+n_b-2} h_{l+m} u_{l+m} \quad (49)$$

with $n_{a,b}$ denoting the respective protein sizes. We allow the fields h_n to depend on the site. Discrete Fourier transform gives

$$H = \frac{1}{2N} \sum_q \tilde{K}_q |\mathcal{U}_q|^2 - \frac{1}{N} \sum_q \left(C_q + e^{2\pi i m q/N} D_q \right) \mathcal{U}_q \quad (50)$$

with

$$C_q = \sum_{k=0}^{n_a-1} h_k e^{2\pi i k q/N} \quad (51)$$

$$D_q = \sum_{l=n_a-1}^{n_a+n_b-2} h_{l+m} e^{2\pi i l q/N} \quad (52)$$

Using the definition

$$h_q^* \equiv C_q + e^{2\pi i m q/N} D_q \quad (53)$$

we can rewrite (50) as

$$\begin{aligned} H &= \frac{1}{2N} \sum_q \tilde{K}_q |\mathcal{U}_q|^2 - \frac{1}{2N} \sum_q (h_q^* \mathcal{U}_q + h_q \mathcal{U}_q^*) \\ &= \frac{1}{2N} \sum_q \tilde{K}_q |\mathcal{U}_q|^2 - \frac{1}{2N} \sum_q \frac{|h_q|^2}{\tilde{K}_q} \end{aligned} \quad (54)$$

where we have defined

$$\mathcal{U}'_q = \mathcal{U}_q - \frac{h_q}{\tilde{K}_q} \quad (55)$$

To get the partition function we integrate on \mathcal{U}'_q . The integration of the term $|\mathcal{U}'_q|^2$ gives F_0 the free energy of the DNA. The second term in (54) contributes to the excess free energies $\Delta F_a + \Delta F_b + \Delta \Delta F_{int}$. Expressing $|h_q|^2$ in terms of C_q and D_q we find

$$\begin{aligned} F_{ab} &= F_0 - \frac{1}{2N} \sum_q \frac{|C_q|^2 + |D_q|^2}{\tilde{K}_q} \\ &\quad - \frac{1}{2N} \sum_q \frac{C_q D_{-q} + C_{-q} D_q}{\tilde{K}_q} e^{2\pi i m q/N} \end{aligned} \quad (56)$$

where we used the relations $C_q^* = C_{-q}$ and $D_q^* = D_{-q}$. The terms proportional to $|C_q|^2$ and $|D_q|^2$ are ΔF_a and ΔF_b . The interaction term itself is given by:

$$\Delta \Delta F_{int} = -\frac{1}{2N} \sum_q \frac{C_q D_{-q} + C_{-q} D_q}{\tilde{K}_q} e^{2\pi i m q/N} \quad (57)$$

The localized perturbation limit, e.g. $-h(u_0 + u_m)$, discussed in the main text is obtained by setting $n_a = n_b = 1$ and $h_0 = h_m = h$ in the two sums in (51) (52), which corresponds to $C_q = D_q = h$ and hence

$$\Delta \Delta F_{int} = -\frac{h^2}{N} \sum_q \frac{e^{2\pi i m q/N}}{\tilde{K}_q} \quad (58)$$

which is Eq. (11) of the main text. We find therefore that an extended linear perturbation generates a q -dependent term $C_q D_{-q} + C_{-q} D_q$ in the sum (57). This does not modify the analytical structure of the leading poles, unless $C_q D_{-q} + C_{-q} D_q$ vanishes at $q = q_E$ as well, a very peculiar limiting case which we exclude from our analysis. The conclusion is that the extended perturbation (49) generates the same asymptotic damped oscillatory decay as the localized perturbation discussed in the text (66). This decay is thus robust.

2. Entropic and mixed allostery: lack of robustness of oscillations

To test the effect of an extended coupling on entropic allostery we consider

$$H = H_0 + \varepsilon (u_0^2 + u_1^2 + u_{m+1}^2) \quad (59)$$

We omit the details of the calculation which consists in computing the probability distribution of three variables $p(u_0, u_1, u_{m+1})$ which generalizes (18). One then computes the interaction free energy as done above for the other cases. The final result is

$$\Delta\Delta F_{int} = \frac{k_B T}{2} \log \left(1 - \frac{4\varepsilon^2 [1 + 2\varepsilon(S_0 - S_1)] (S_{m+1}^2 + S_m^2) + 8\varepsilon^3 S_1 (S_{m+1} - S_m)^2}{[1 + 4\varepsilon^2 (S_0^2 - S_1^2) + 4\varepsilon S_0] (1 + 2\varepsilon S_0)} \right) \quad (60)$$

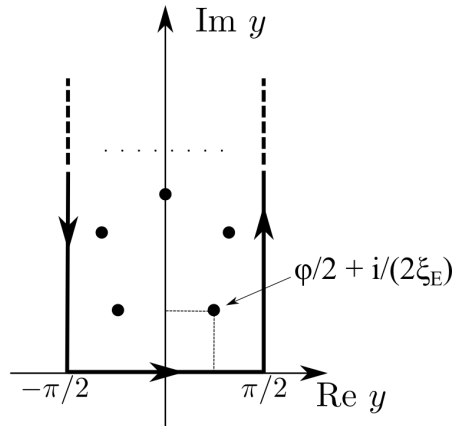


FIG. 5. Solid line: Integration contour for the calculation of the integral (64). Circles: poles of the integrand obtained by solving $\tilde{K}_q = 0$ (here $y \equiv \pi q/N$). We note that \tilde{K}_q is an even function of q . The leading large m behavior is due to the pole(s) closest to the $Re(y)$ axis, is indicated with an arrow.

We note that we can formally recover Eq. (40) (which we report here for convenience)

$$\Delta\Delta F_{int} = \frac{k_B T}{2} \log \left[1 - \left(\frac{2\varepsilon S_m}{1 + 2\varepsilon S_0} \right)^2 \right] \quad (61)$$

by setting $S_1 = S_{m+1} = 0$ in (60). Also (60) describes a stabilizing interaction $\Delta\Delta F_{int} \leq 0$. The main difference in the two cases is that, while (61) vanishes whenever $S_m = 0$ and thus has the same zeros as the enthalpic case, in (60) this does no longer happen. The m -dependence of the interaction comes from terms proportional to S_m^2 , S_{m+1}^2 and $S_m S_{m+1}$. The combination of these gives an overall exponential decay $\exp(-2m/\xi_E)$ with products of cosines of different phases which suppress the oscillating part. The numerical solution of the general case

$$H = H_0 + \sum_{k=0}^{n_a-1} \varepsilon_k u_k^2 + \sum_{l=n_a+1}^{n_a+n_b-2} \varepsilon_{m+l} u_{m+l}^2 \quad (62)$$

shows that oscillating components get more and more suppressed as the number of interacting sites increases (larger n_a and n_b), see Fig. 2(b) in the main text. Summarizing we expect for this case an asymptotic behavior of the type

$$\Delta\Delta F_{int} \sim f(m) e^{-2m/\xi_E} \quad (63)$$

with $f(m)$ a very weak function of m . A very similar behavior holds for the mixed case (see Fig. 2(c) in the main text).

II. ALLOSTERIC LENGTH SCALE

A. The propagator and its asymptotics

In the limit $N \rightarrow \infty$ we can transform the discrete sum defining the propagator S_m (22) into an integral

$$S_m = \frac{1}{N} \sum_q \frac{e^{2\pi i m q/N}}{\tilde{K}_q} = \frac{1}{\pi} \int_{-\pi/2}^{\pi/2} \frac{e^{2im y} dy}{\sum_n K_n \cos(2ny)} \quad (64)$$

where we used the change of variable $y \equiv \pi q/N$ and the expression for \tilde{K}_q in (4). To evaluate the integral one closes the integration domain in the complex y -plane, as shown in Fig. 5. Integrals along the two vertical lines cancel each other by symmetry. The leading large- m contribution comes from the poles in the integrand with the smallest imaginary part (closest to the $Re(y)$ axis). There cannot be poles on the real axis, as this would lead to $\tilde{K}_q = 0$ for some real q , hence an instability for that mode. Indicating the leading poles with

$$y_{\pm} = \pm \frac{\phi}{2} + \frac{i}{2\xi_E} \quad (65)$$

and defining $g(y) \equiv \sum_n K_n \cos(2ny)$ one gets in the asymptotic limit ($m \gg 1$)

$$S_m \sim 2i \left[\frac{e^{2im y_+}}{g'(y_+)} + \frac{e^{2im y_-}}{g'(y_-)} \right] \quad (66)$$

Defining $g'(y_+) = C_1 + iC_2$ and using the relation $g'(y_+) = -[g'(y_-)]^*$ one has $g'(y_-) = -C_1 + iC_2$ which gives Eq.(9) of the main text

$$S_m \sim \Gamma \cos(m\phi + \phi_0) e^{-m/\xi_E} \quad (67)$$

where

$$\Gamma = \frac{4}{\sqrt{C_1^2 + C_2^2}} \quad \cos \phi_0 = \frac{C_2}{\sqrt{C_1^2 + C_2^2}} \quad (68)$$

1. Some examples of \tilde{K}_q

The values of ϕ and ξ_E depend on the interaction parameters K_n . As a simple analytically solvable example we consider only one non-local term ($K_1 \neq 0$)

$$\tilde{K}_q = K_0 + K_1 \cos\left(\frac{2\pi q}{N}\right) \quad (69)$$

i.e. setting $K_l = 0$ for $l \geq 2$. The stability condition $\tilde{K}_q > 0$ for real q imposes $|K_1| < K_0$. There are thus two

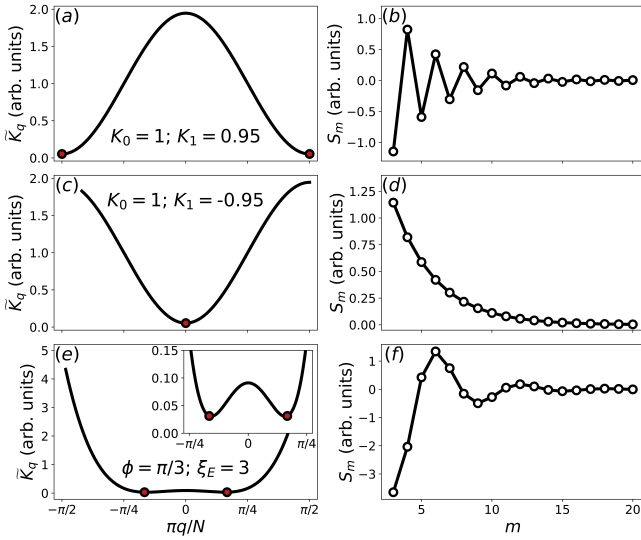


FIG. 6. Examples of \tilde{K}_q (left columns) with the corresponding propagators S_m vs. m (right columns). The real parts of the poles of \tilde{K}_q are shown in (a,c,d) as red circles. (a-d) correspond to a model with a single distal coupling K_1 , with \tilde{K}_q given in Eq. (69) and $K_1 > 0$ (a-b), $K_1 < 0$ (c-d). In the case (a) the leading pole has a non-vanishing real component ($\phi = \pm\pi$) which produces oscillations with the highest possible frequency in the propagator $S_m \sim (-1)^m e^{-m/\xi}$, shown in (b). In the case (c) the leading pole has a vanishing real part ($\phi = 0$), which gives a monotonic decay $S_m \sim e^{-m/\xi}$, shown in (d). The case (e) corresponds to the continuum model (73). The real part of the pole $\text{Re}(q_E)$ is close to the minimum of \tilde{K}_q . Coarse-grained variables characterized by stiffnesses as in (a) and (c) cannot be responsible for allosteric effects seen in DNA experiments, as they do not produce the damped oscillatory behavior.

cases with K_1 positive or negative as shown in Fig. 6(a) and (c). Defining $\omega \equiv \exp(2\pi i q/N)$ one has

$$\cos\left(\frac{2\pi q}{N}\right) = \frac{1}{2} \left(\omega + \frac{1}{\omega} \right) \quad (70)$$

and $\tilde{K}_q = 0$ becomes a second degree equation for ω which give a single pole. For $0 < K_1 < K_0$ the pole is

$$\phi = \pm\pi, \quad \frac{1}{\xi_E} = \log\left(\frac{K_0 + \sqrt{K_0^2 - K_1^2}}{K_1}\right) \quad (71)$$

while for $-K_0 < K_1 < 0$ the pole is

$$\phi = 0, \quad \frac{1}{\xi_E} = \log\left(\frac{K_0 + \sqrt{K_0^2 - K_1^2}}{|K_1|}\right) \quad (72)$$

We note that in both cases $\xi_E \rightarrow 0$ as $K_1 \rightarrow 0$, as allostery requires some off-site couplings. Moreover the allosteric length diverges as $|K_1| \rightarrow K_0$. In this limit the minimum $\min_q(\tilde{K}_q) \rightarrow 0$, the corresponding mode q^* of the leading pole becoming unstable. In more complex

situations, with further neighbor couplings one needs to solve $\tilde{K}_q = 0$ numerically, as this equation is a higher degree polynomial in the variable ω .

In the main text we introduced a minimal model for allostery with a \tilde{K}_q given by

$$\tilde{K}_q = C (q^2 - q_E^2) (q^2 - q_E^{*2}) = C (q^4 - 2\mu q^2 + \lambda) \quad (73)$$

with $\mu = q_E^2 + q_E^{*2} > 0$, $\lambda = |q_E|^4 > 0$ and C a constant. The quartic model (73) is plotted in Fig. 6(e). This model is based on a \tilde{K}_q having a minimal number of zeros. Symmetry requires minimal four such zeros, hence a polynomial of degree four. We note that (73) is not a combination of cosines as in Eq. (4) of the main text. It describes instead a continuum model with energy:

$$H_0 = C \int_0^L ds \left[(\partial_s^2 u(s))^2 - 2\mu (\partial_s u(s))^2 + \lambda u^2(s) \right] \quad (74)$$

with $0 \leq s \leq L$ continuous coordinate (replacing the base pair index) and L the total length of the DNA. The right column of Fig. 6 shows plots of the propagators S_m vs. m corresponding to the stiffnesses shown in the left column. As allosteric effects manifest themselves in experiments as damped oscillations, the associated stiffness is expected to be as in Fig. 6(e).

B. Distal couplings in DNA models

The DNA-mediated allostery discussed in this paper is due to non-vanishing distal couplings. Such couplings have been observed in simulations by various groups [10–14, 18, 19]. Their origin is twofold. Firstly, the coarsening of local degrees of freedom leads to coarse-grained variables with couplings that extend beyond nearest neighbors. Secondly, DNA interacts in a complex way with solvent and counterions which leads to interactions which extend beyond neighboring bases.

The ordinary Twistable Wormlike Chain (TWLC) model, which describes DNA deformations using twist and bending degrees of freedom, is a very good model of DNA mechanics at sufficiently long length scales (~ 100 bp and beyond). Such model is strictly local and does not have distal couplings, therefore it is not suitable to describe DNA at a local scale where such couplings have been observed (~ 10 bp). Figure 7 shows the Fourier space stiffness of *bending* and *twist* modes as obtained from all-atom simulations. The q -dependence indicates the presence of distal couplings. The stiffnesses have a global maximum at $q = 0$ and minima at $q = \pm N/2$ and are of the type shown in Fig. 6(a). As a consequence, the correlation functions of twist or bend deformations decay with alternating signs, as shown in Fig. 6(b). The characteristic correlation lengths was estimated to be $\xi \approx 4$ bp [19]. Such degrees of freedom cannot produce an oscillatory coupling free energy with the double helical period, as observed in DNA allostery experiments [3]. We can

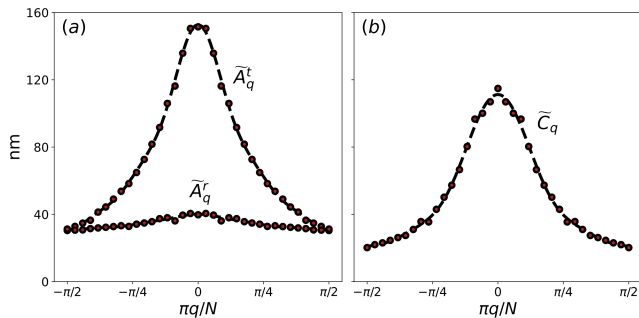


FIG. 7. Red circles: Fourier space stiffnesses for (a) bending deformations (tilt \tilde{A}_q^t and roll \tilde{A}_q^r) and (b) twist deformation \tilde{C}_q , as obtained from all atom simulations averaging two different sequences of 44-mers of DNA. Note that the very different behavior of the two bending stiffnesses of Fig. 7(a): tilt has a very strong q -dependence, while this is very weak in roll. This peculiar feature was discussed in [36]. Dashed lines: Fourier decomposition of the stiffnesses. The correlators S_m associated to these degrees of freedom alternate in sign as shown in Fig. 6(b). Such a behavior is not consistent with the oscillatory decay of DNA allostery observed in experiment. Hence allosteric interactions are unlikely to be carried by pure bending or twist deformations.

therefore conclude that DNA allostery is unlikely to be carried by pure twist and bending deformations.

In principle there are several other degrees of freedom describing DNA deformations at the base pair level. A popular coarse grained model, the rigid base model, introduces 12 degrees of freedom per site (6 intra-basepair and 6 inter-basepair, see e.g. [20]). In such model DNA bases A,T,C,G are treated as rigid bodies while translation vectors and rotation angles are used to parametrize their relative positions and orientations. The degrees of freedom describing conformations of the rigid base model are also characterized by non-local couplings and therefore have associated correlation lengths (as shown by Eqs. (71) and (72) a single non-zero distal coupling is sufficient to induce a correlation length). The oscillating interaction observed in experiments puts a constraint on the coarse-grained variables acting as carriers of the allosteric coupling. Such variables must necessarily have a stiffness of the type of Fig. 6(e). The analysis of simulation data indicates that the major-groove width has the double-well shaped stiffness which can potentially generate such oscillating decaying interactions. Our model is quadratic in the variables u_n . Some proteins are known to physically modify the DNA rather strongly so that anharmonic effects may become relevant. There is currently little known about anharmonic effects in DNA. These were recently explored for some degrees of freedom [19], although the analysis is far from complete. In that paper a novel biasing scheme was introduced to investigate strongly deformed DNA in all-atom simulations. The biasing is necessary as in unconstrained simulations one does not observe anharmonic effects just from

thermal fluctuations. Some degrees of freedom, such as twist, were found to behave harmonically for a range to ± 10 degrees per base pair (see Fig. 2 of [19]), which is a rather large value considering it affects only two consecutive base pairs. Anharmonic effects could be relevant in the enthalpic case as a quadratic perturbation $\sim u_m^2$ in our model suppresses fluctuations, thereby keeping the DNA deformations within the harmonic regime. The enthalpic case with strongly DNA deforming proteins will be analyzed in future work.

C. Allosteric lengths vs. persistence lengths

In principle any local degree of freedom with distal couplings has an associated allosteric length ξ_E . The long length scale behavior of the DNA is described by torsional and bending persistence lengths. The allosteric length is however unrelated to these persistence lengths as it can be best illustrated using torsional elasticity as an example. The energy (in rescaled $k_B T$ units) is

$$\begin{aligned} \beta H_{\text{twist}} &= \frac{a}{2} \sum_{n=0}^{N-1} \left[C_0 \Omega_n^2 + \sum_{p=1}^L C_p (\Omega_n \Omega_{n+p} + \Omega_n \Omega_{n-p}) \right] \\ &= \frac{a}{2N} \sum_q \tilde{C}_q |\tilde{\Omega}_q|^2, \end{aligned} \quad (75)$$

where Ω_n is the excess twist per unit length between the two consecutive base pairs n and $n+1$ and a is a discretization length corresponding to the distance between base pairs ($a = 0.34 \text{ nm}$). C_p indicate the stiffnesses and the (75) is the same for as that in the manuscript for the variable u_n . The torsional correlation function is given by (see details in [13])

$$\left\langle \cos \left(a \sum_{n=0}^{m-1} \Omega_n \right) \right\rangle \stackrel{m \gg 1}{\sim} e^{-ma/\xi_T}, \quad (76)$$

with

$$\xi_T = 2\tilde{C}_0 = 2 \sum_{p=-L}^L C_p. \quad (77)$$

The calculation was done for correlated variables and it is a bit more complex than for the usual Twistable Wormlike Chain (TWLC) where bending and twist at different sites are uncorrelated. Hence in the model (75) the ordinary torsional correlation length is related to the $q=0$ (long wavelength limit) of the Fourier transform of the couplings. This can also be seen in the torque ensemble where the energy becomes:

$$\begin{aligned} \beta H &= \beta H_{\text{twist}} - \beta \tau a \sum_{n=0}^{N-1} \Omega_n \\ &= \frac{a\tilde{C}_0}{2N} \tilde{\Omega}_0^2 - \beta \tau a \tilde{\Omega}_0 + \frac{a}{2N} \sum_{q \neq 0} \tilde{C}_q |\tilde{\Omega}_q|^2 \end{aligned} \quad (78)$$

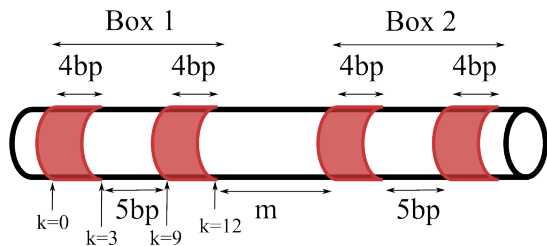


FIG. 8. Schematic view of the structure of the ComK-DNA binding interface (red dashed area). There are two “binding boxes” separated by a linker of m base-pairs. Each box consists of two regions of fixed sequence of four base pairs each, separated by a 5 bp variable region. Two proteins bind at each binding box, so allostery involves in total four ComK. We model the proteins binding in each box using linear and quadratic fields in each of the 8 binding sites, as given in Eq. (80). The 4 bp DNA sequences are mirror symmetric, hence we use the same field values at sites $k = 0, 12$, $k = 1, 11$, $k = 2, 10$ and $k = 3, 9$.

which shows that the torque τ couples only to the mode $q = 0$. The torque response is governed again by the $q = 0$ component of the stiffness \tilde{C}_q .

The allosteric effects we discussed in this paper are instead linked to the correlator

$$\langle \Omega_n \Omega_{n+m} \rangle \stackrel{m \gg 1}{\approx} e^{-ma/\xi_E} \quad (79)$$

where ξ_E is determined from the leading (complex) solution of $\tilde{C}_q = 0$. ξ_T and ξ_E are therefore two distinct length scales, both linked to \tilde{C}_q . From experiments probing DNA mechanical properties we know that $\xi_T \approx 200 \text{ nm} = 600 \text{ bp}$. The other lengthscale is expected to be of the order of a few base pairs $\xi_E \approx 5 \text{ bp}$ [13]. The ordinary TWLC, considered the standard DNA model, describes DNA as uncorrelated twist and bending variables. It is a valid description at length scales $\gg \xi_E$. The previous discussion for simplicity was limited to twist, but for every local variable u_n there is an associated correlation length ξ_E , defined from correlation functions as (79).

III. FITTING PROCEDURE OF COMK DATA

We discuss here the procedure used to fit the ComK data of Fig. 3(b) of the main text. The comK binding sites consists of two boxes as shown in Fig. 8. Each box has two 4 bp regions of conserved sequences throughout various organisms, which are separated by a variable 5 bp tract [4]. Two ComK molecules bind to each binding box, so that in total four ComK are involved in the allosteric communication [4]. To fit the experimental data, we model the binding of a first pair of ComK molecules at a binding box by two extended perturbations each spanning over four sites in order to assimilate the length of the binding domains within one box. The perturbations are placed at a fixed distance of five sites from one

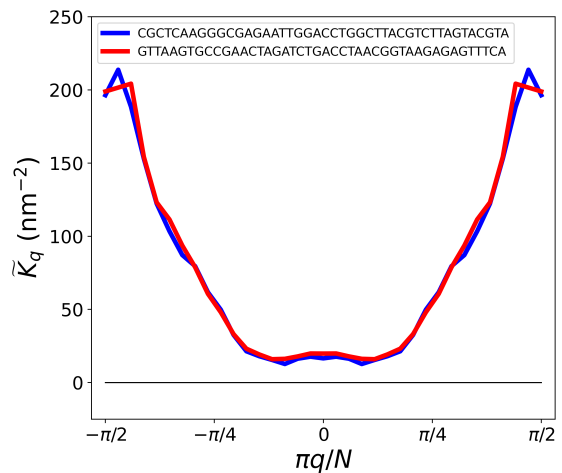


FIG. 9. Plot of the momentum-space stiffness for the major groove width obtained from all-atom simulations for two oligomers of 44 bps. The two sequences are given in the top of the figure.

another accounting for the five base-pairs between binding domains. Each of the individual perturbations entails a linear field (h_0, h_1, h_2, h_3) and a quadratic field ($\epsilon_0, \epsilon_1, \epsilon_2, \epsilon_3$) such that the free energy of DNA bound to a single pair of ComK is given by:

$$H = H_0 + \sum_{k=0}^3 [\epsilon_k (u_k^2 + u_{12-k}^2) - h_k (u_k + u_{12-k})] \quad (80)$$

Where the $12-k$ accounts for the anti-symmetric binding of the two ComK molecules. The binding of a second pair of ComK proteins is modelled by the same perturbation displaced over a distance of m sites. For a given combination of h_k and ϵ_k , $\Delta\Delta F_{int}(m)$ is calculated numerically. In order to find an appropriate choice of h_k and ϵ_k fitting the data we implemented a Monte Carlo algorithm. During each MC step h_k and ϵ_k are altered after which the change is accepted/rejected based on the Metropolis acceptance criterion. Due to the presence of linear and quadratic fields the interaction free energy is comprised of an energetic (Enthalpic and Mixed allostery) and an entropic component. We allow for the entropic term to be multiplied by an integer prefactor reflecting the relevance of several degrees of freedom in DNA-ComK binding.

IV. ALL ATOM SIMULATIONS

All simulations were done using version 2020.4 of Gromacs [21] and the Amberff99 parmbsc1 force field (based on the parm99 forcefield, improved with bsc0 [22] corrections and bsc1 corrections [23]). Water was modelled using the TIP-3P model [24] non-bonded interactions were cutoff at 1.0 nm and PME Mesh Ewald interactions

	K_0	K_1	K_2	K_3	K_4	K_5
\tilde{K}_q (major-groove width)	77	-43	15	-3.5	3.8	-1.2
\tilde{A}_q^t (tilt)	74	26	7.3	4.0	1.5	0.9
\tilde{A}_q^r (roll)	35	2	0.4	0.2	0.01	0.1
\tilde{C}_q (twist)	53	20	6.6	2.3	0.2	-0.1

TABLE I. Real space stiffnesses K_m for the major-groove width \tilde{K}_q , tilt \tilde{A}_q^t , roll \tilde{A}_q^r and twist \tilde{C}_q . Values are obtained by fitting the q-stiffnesses extracted from all-atom data (see Figures 4 and 7) with Eq. 3. In contrast to bending and twist deformations, the off-site couplings K_p for the major-groove width have alternating signs, giving rise to the distinctive double-welled shape of \tilde{K}_q .

was used for electrostatics. Simulations started from two 44bp random sequences. The starting configuration was generated using 3DNA [25]. The DNA molecules were placed into a dodecahedral box, leaving 2.0 nm on either side of the molecule, with periodic boundary conditions and solvated in a 150 mM NaCl solution after which the overall charge in the system was neutralised. This structure was energy minimised with a tolerance of 1000 kJ/mol to make sure no overlap remained between solvent molecules and DNA. Subsequently, the molecule was equilibrated in the NVT ensemble for 100 ps where temperature was kept at 300 K using a velocity rescaling thermostat [26] and then equilibrated for another 100 ps in the NPT ensemble at the same temperature but using a Parrinello-Rahman barostat [27] to fix the pressure at 1.0 bar. Production runs were performed under the same conditions for 100 ns for each sequence. All simulations were performed using a 2 fs time step in a leapfrog integrator, using LINCS [28] to constrain the covalent bonds involving hydrogen atoms. Afterwards the tra-

jectories were analyzed and the groove widths extracted using Curves+ [35].

Figure 9 shows the \tilde{K}_q as calculated from the two individual 44-mers random sequences. The stiffness is weakly dependent on the sequence, suggesting the groove width deformations can be approximately described by a homogeneous model. The sequence to sequence variation for bending and twist deformation is typically much stronger, see simulation data in [13]. We report in Table I the local stiffness (K_0) and the distal couplings (K_1 , K_2 , $K_3 \dots$) as obtained from all atom simulations data analysis for major groove width, tilt, roll and twist coordinates.

To produce a propagator S_m with a monotonic decay or a decay with alternating signs (as those shown in Fig. 6 (b) and (d)) a single distal coupling $K_1 \neq 0$ is sufficient. One can think about the equivalent problem in the one-dimensional ferromagnetic or antiferromagnetic Ising model with nearest-neighbor coupling. Equations (71) and (72) give the analytical expressions of ξ_E in these two cases. To produce damped oscillations with the period of the double helix longer range couplings are necessary. It is likely that all-atom simulations do not reproduce these types of effects because of either limitations in the reachable timescales ($\sim \mu s$) or because of problems with the parametrization. Current all-atom DNA models are parametrized using classical force fields which have some shortcomings, as discussed recently in [29]. One of the conclusions of that paper is that current state-of-the-art force fields overstabilize nucleic acids suppressing possible “higher degree conformational transitions”. These conformational changes may lead to stronger correlation effects and thus to closer agreement with allostery experiments. There is an ongoing effort to develop more accurate force fields for nucleic acids [29] and allostery data could be used as test case.